Physics Letters B ••• (••••) ••••••

Contents lists available at ScienceDirect

Physics Letters B

www.elsevier.com/locate/physletb

Solar neutrino scattering with electron into massive sterile neutrino

Shao-Feng Ge [a], Pedro Pasquini [a], Jie Sheng [a,b]

[a] Tsung-Dao Lee Institute & School of Physics and Astronomy, Shanghai Jiao Tong University, China
[b] Physics Department, Jilin University, Changchun, Jilin Province, China

ARTICLE INFO

Article history:
Received 13 July 2020
Accepted 13 September 2020
Available online xxxx
Editor: J. Hisano

ABSTRACT

The recent Xenon1T excess can be explained by solar neutrino scattering with electron via a light mediator, either scalar or vector, in addition to many other explanations from the dark sector. Since only the recoil electron is observable, a keV sterile neutrino instead of an active neutrino can appear in the final state. The sterile neutrino allows pseudoscalar mediator to explain the Xenon1T excess which was thought impossible. In addition, nonzero recoil energy lower bound arises from the sterile neutrino mass, which can be used to testify if the sterile neutrino is massive or not. We also briefly discuss the case of sterile neutrino final state with light Z' mediator.

1. Introduction

The recent Xenon1T data contains a low-energy peak excess in the electron recoil spectrum [1]. Although it is possible to explain this peak excess with residual tritium background [1,2], more data or independent measurement is needed before making a decisive conclusion. It is too soon to call this Xenon1T signal an anomaly. On the other hand, this low energy peak can also be explained with new physics beyond the Standard Model (SM).

The largest category is dark sector which contains several possibilities. To explain the observed low-energy excess with dark matter (DM), [3] pointed out that the DM has to move faster, $v \gtrsim 0.05$, than the conventional non-relativistic DM confined in our galaxy, which typically has velocity $v \sim 10^{-3}$ ($\mathcal{O}(100\,\mathrm{km/s})$. This is followed by many attempts in various scenarios, including boosted DM [4], cosmic-ray boosted DM [5–7], inelastic cosmic-ray boosted DM [8], warm DM decay [9], DM heated in the Sun [10], inelastic DM-electron scattering from heavy to light [11,12], inelastic DM-electron scattering from light to heavy [13], $2 \to 4$ annihilating DM [14], $3 \to 2$ Co-SIMP DM [15], shinning DM emitting photon to fake electron recoil with Rayleigh operator [16], electromagnetic de-excitation [17], Migdal effect with electron signal from nuclei recoil [18], mirror DM [19], and Hydrogen atom decay [20]. There is also some discussion about using collider search to supplement the direct detection [21]. Although the solar axion explanation is in tension with astrophysical constraints [1,22], reexamination shows new possibility [23–26] and axion-like-particle (ALP) dark matter is much less constrained [24,27,28]. The light boson category also includes relaxion [29] and dark photon [30–33].

The electron recoil by solar neutrinos is also a major category. Large magnetic momentum from the Majorana nature of neutrinos [34,35] has also being used to explain the Xenon1T excess [1,36,37]. In addition to the photon mediator, either a light scalar [36,38] or Z' [36,38–41] is needed. Although the neutrino charge radius [36] and muon magnetic momentum [42] was additionally studied, they can only provide a quite flat recoil spectrum and hence cannot explain the Xenon1T excess. It is a common feature of having light mediators for the solar neutrino explanations. Both scalar and vector mediators have been discussed. And it is explicitly claimed that the pseudoscalar mediator does not work [38] due to lack of low recoil enhancement [29,38], which is not necessarily true.

We propose a new possibility with sterile neutrino in the final state, in addition to the light mediator. It allows pseudoscalar to provide a $1/T_r$ enhancement at low energy and hence can explain the Xenon1T excess. In addition, the finite mass of the sterile neutrino leads to a sharp cutoff on the lower side of the electron recoil spectrum for fixed neutrino energy. This provides the DM direct detection experiments a chance of not just probing the existence of DM but also measuring the companion particle mass. The same scenario also applies for a light Z' mediator as we briefly discuss at end.

E-mail addresses: gesf@sjtu.edu.cn (S.-F. Ge), ppasquini@sjtu.edu.cn (P. Pasquini), shengjie.physics@gmail.com (J. Sheng).

https://doi.org/10.1016/j.physletb.2020.135787

2. Sterile neutrino and light mediator

Let us consider a light scalar mediator with both neutrino and electron,

$$\mathcal{L}_{\rm int} = \bar{\nu}(y_S^\nu + \gamma_5 y_P^\nu)\phi\nu_s + \bar{e}(y_S^e + \gamma_5 y_P^e)e\phi + h.c., \tag{1}$$

with both scalar and pseudoscalar couplings to keep general. This kind of coupling can arise from the mixing of scalar ϕ with the SM Higgs. The Yukawa term requires a right-handed neutrino that has no SM gauge interactions and hence is a sterile neutrino. It is possible for this sterile neutrino to obtain a Majorana mass term. The sterile neutrino ν_s has mass $m_s \sim O(100\,\text{keV})$ and the scalar mediator ϕ has mass $m_\phi \lesssim 30\,\text{keV}$.

When scattering with electron, the light mediator would introduce a $1/(q^2 - m_\phi^2)$ propagator. If the mediator is light enough, $m_\phi^2 \ll q^2 = 2m_e T_r$, $1/T_r$ enhancement at low energy naturally appears. The Xenon1T peak excess, $T_r \approx (2 \sim 3)\,\text{keV}$, corresponds to $m_\phi \ll (40 \sim 60)\,\text{keV}$. Nevertheless, whether the differential cross section has such feature or not is still subject to the scattering matrix element $\overline{|\mathcal{M}|^2}$ [44],

$$4m_e(2m_e T_r + m_s^2)\frac{(y_S^\nu y_S^e)^2(2m_e + T_r) + (y_P^\nu y_P^e)^2 T_r}{(2m_e T_r + m_\phi^2)^2}. \tag{2}$$

The first term in the numerator is the scalar contribution while the second one comes from the pseudoscalar coupling. The difference formally emerges from the electron spinor trace.

$$\text{Scalar}: |\mathcal{M}|^2 \propto \text{Tr}\left[(\not{p}_e + m_e)(\not{p}'_e + m_e)\right], \tag{3a}$$

$$\text{Pseudoscalar}: |\mathcal{M}|^2 \propto \text{Tr}\left[(\not{p}_e + m_e)\gamma_5(\not{p}'_e + m_e)\gamma_5\right]. \tag{3b}$$

Due to the presence of γ_5, the scalar matrix element (3a) becomes $4(m_e^2 + p_e \cdot p'_e)$ while the pseudoscalar one is $4(m_e^2 - p_e \cdot p'_e)$ instead. With $p_e \cdot p'_e = m_e(T_r + m_e)$. Hence, the scalar and pseudoscalar terms become $4m_e(2m_e + T_r)$ and $4m_e T_r$, respectively. The pseudoscalar terms scales linearly with T_r while the scalar one is almost flat.

The scalar and pseudoscalar couplings contribute separately. To see the features of this new interaction in (2) more clearly, let us first omit the mediator mass m_ϕ and take $2m_e \gg T_r$ into consideration. For a light sterile neutrino, $2m_e T_r \gg m_s^2$, the scalar term has $1/T_r$ peak while the pseudoscalar one becomes almost independent of the electron recoil energy. For light final state such as the active neutrinos in the SM, the pseudoscalar mediator can not explain the Xenon1T excess [38,45].

Nevertheless, this conclusion is not necessarily true in the presence of final-state sterile neutrino. For $m_s^2 \gtrsim 2m_e T_r$, the prefactor $2m_e T_r + m_s^2 \approx m_s^2$ in (2) no longer has linear dependence on the electron recoil energy T_r but becomes almost flat. This introduces $1/T_r$ to the pseudoscalar contribution and enhance the scalar one to $1/T_r^2$. In addition to the energy recoil peak introduced by a light mediator that one usually expects, a massive final state can do the same thing. The scenario of hidden neutrino in the final state [39] with mass at sub-eV scale and a Z' mediator is quite different from the one we consider here.

From the scattering matrix element $\overline{|\mathcal{M}|^2}$ to the differential cross section $d\sigma/dT_r$,

$$(2m_e T_r + m_s^2)\frac{(y_S^\nu y_S^e)^2(2m_e + T_r) + (y_P^\nu y_P^e)^2 T_r}{8\pi E_\nu^2 (2m_e T_r + m_\phi^2)^2}, \tag{4}$$

no extra T_r is introduced. We show the electron recoil energy spectrum in Fig. 1 which clearly demonstrates a surging peak at low energy. The SM contribution is mainly from the heavy Z and W mediators with flat recoil spectrum [46]. The blue curve for scalar and massless neutrino in the final state roughly overlaps with the dashed curve for pseudoscalar curve with $m_s = 100\,\text{keV}$ due to the $1/T_r$ dependence as we elaborated above. If the final-state neutrino is also massive, the scalar contribution receives one more $1/T_r$ enhancement and leads to the black curve in Fig. 1, which shows clearly the effect of a massive sterile neutrino in explaining the low-energy recoil signal observed by Xenon1T.

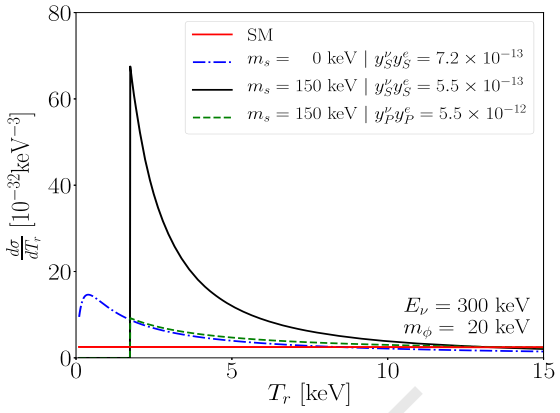

Fig. 1. The electron recoil energy spectrum for the SM background and sterile neutrino final state with scalar mediator.

The sterile neutrino as DM can also introduce a peak in the low energy recoil spectrum [43]. The mass of the sterile neutrino in the initial state is converted to kinetic energy of the final-state particles. With sterile neutrino mass, $m_s \lesssim 40$ keV, the electron recoil energy receives a natural upper limit at the keV scale and hence a peak. In this scenario, there is no need to involve a light mediator and the SM Z boson mediation is enough to explain the low energy peak.

3. Solar neutrino

We used the NuPro package [47] to simulate the evolution [48,50] of solar neutrinos [49,51,52]. The solar neutrinos are produced from the *pp* chain and CNO cycle nuclear reactions according to which the neutrino fluxes can be predicted [53]. In total, there are 6 continuous fluxes (*pp*, ^{13}N, ^{16}O, ^{17}N, ^{8}B, and *hep*) and 3 monoenergetic ones (the ^{7}B flux has 10.44% at 384 keV and 89.56% at 862 keV, as well as *pep* at 1.44 MeV). The fluxes without flavor transition have been illustrated with solid lines in the upper panel of Fig. 2. Depending on the solar matter density, composition, and temperature, the production rate varies inside the Sun. Due to the extremely high density inside the Sun, solar neutrinos evolve adiabatically when propagating out and the transition probability P_{ee} depends on the neutrino production location. The solar neutrino fluxes that arrive at detector on the Earth is then the one convoluted with transition probabilities, illustrated as dashed lines in Fig. 2. These effects have been properly taken into account in NuPro. The lower panel of Fig. 2 shows the transition probabilities for different fluxes. Between different fluxes, the transition probability varies a lot, especially for the high energy part. In our simulation, the neutrino parameters are assigned to the best-fit values from the latest global fits [54,55].

4. Xenon1T electron recoil signal

The Fig. 3 shows the signal event rates for both scalar and pseudoscalar mediators. The Xenon1T excess is observed in the Science Run 1 (SR1) data set with 0.65 ton·year exposure. Although the recoil energy spectrum has a sharp peak at low energy, we have to consider the finite energy resolution and the detection efficiency [1]. The energy resolution can be parametrized as

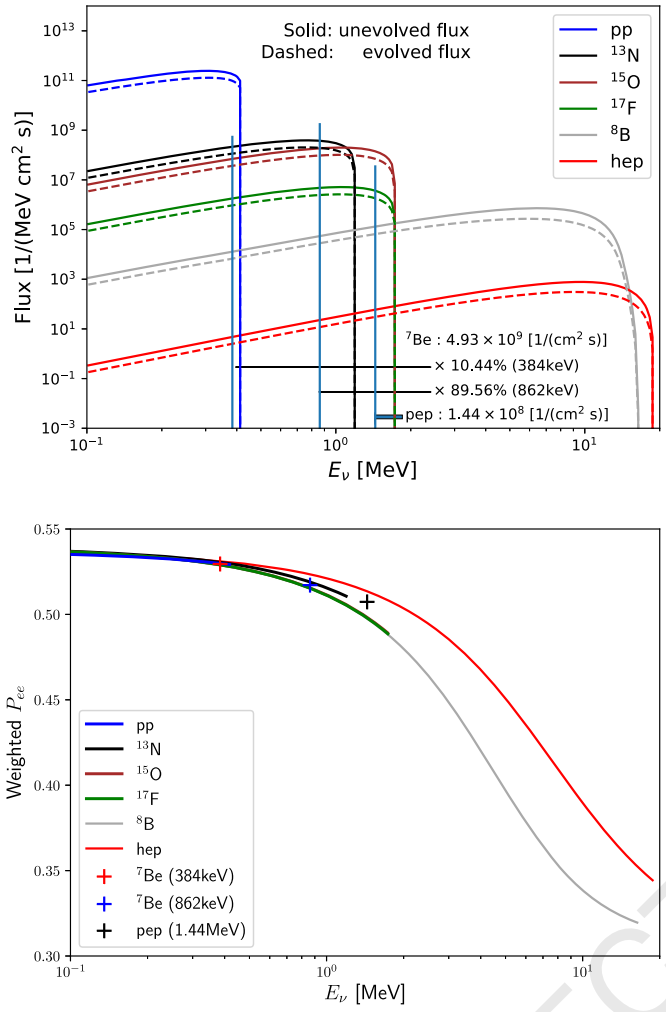

Fig. 2. The solar neutrino fluxes and the transition probabilities.

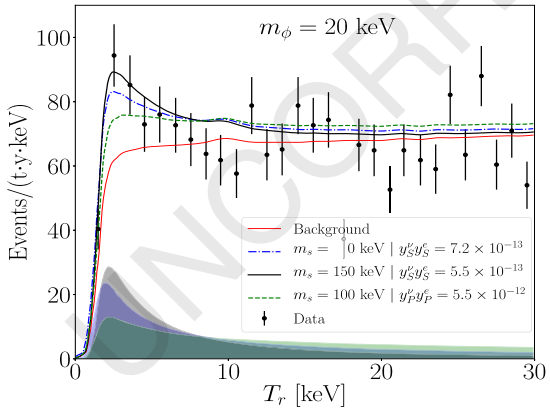

Fig. 3. The electron recoil event rate at Xenon1T.

$\sigma_{T_r} = a/\sqrt{T_r/\text{keV}} + b$ with $a = 31.71 \pm 0.65$ and $b = 0.15 \pm 0.02$ [56]. For simplicity, we just use the central values of a and b. We assign $m_s = 150\,\text{keV}$ for the scalar mediator and $m_s = 100\,\text{keV}$ for the pseudoscalar. In both cases, $m_\phi = 0\,\text{keV}$ can explain the Xenon1T signal.

It should be emphasized that the signal spectrum in Fig. 3 drops faster for a massive sterile neutrino than the massless case. This is because the recoil energy can receive a nonzero lower limit for a massive sterile neutrino final state as indicated in Fig. 1, $T_r^- \le T_r \le T_r^+$ with,

$$T_r^\pm = \frac{1}{2s}\Big\{(s + m_e^2 - m_s^2)E_0 \pm |\mathbf{p}_0|\sqrt{[s-(m_e+m_s)^2][s-(m_e-m_s)^2]}\Big\} - m_e. \tag{5}$$

The center-of-mass energy is, $s = m_e(m_e + 2E_\nu)$, $E_0 = E_\nu + m_e$, and $|\mathbf{p}_0| = E_\nu$. For massless final-state neutrino, $T_r^- = m_e$ and consequently $T_r \ge 0$. In the presence of massive sterile neutrino final state, there is no recoil signal below $T_r^- - m_e$. It is then possible to experimentally justify if the final state companion particle is massless or not. From the gap size low recoil spectrum shape, we may infer the companion particle mass. The electron recoil signal of DM direct detection experiment can not only probe the existence of DM but also the mass of the companion particle. This is not easy at the conventional detectors and new concept detection techniques may help.

5. Interplay with the SM counterparts

In previous discussions, the SM and new physics contributions are essentially independent of each other. Here we try to compare these two contributions by first comparing their sizes and then briefly discuss the possible interference between them.

With the integration limits $T_r^\pm$ in (6), we can readily obtain the total cross section,

$$\sigma = \frac{(y_S^\nu y_S^e)^2}{16\pi m_e E_\nu^2}\left[2m_e \log\frac{T_r^+}{T_r^-} - m_s^2\left(\frac{1}{T_r^+} - \frac{1}{T_r^-}\right)\right] + \frac{(y_P^\nu y_P^e)^2}{32\pi m_e^2 E_\nu^2}\left[2m_e(T_r^+ - T_r^-) + m_s^2 \log\frac{T_r^+}{T_r^-}\right]. \tag{6}$$

A basic feature is the integration limits $T_r^\pm$ scales with neutrino energy E_ν almost linearly for large neutrino energy. Consequently, the total cross section is suppressed for $E_\nu \gg m_e, m_s$ with a $1/E_\nu$ scaling. This behavior is quite different from the SM counterpart [46] which increases linearly with neutrino energy.

In earlier discussions, the SM diagram with active neutrino ν_e in the final state does not interfere with the sterile neutrino contribution due to different final states, one is active neutrino and the other sterile neutrino. This is based on the assumption of ignoring the active-sterile mixing which is always achievable since the existence of sterile neutrino has not been established by neutrino oscillation experiments [57–59], although the decay of a keV neutrino could explain the LSND and MiniBooNE excess [60].

One may imagine the situation that the active-sterile mixing can introduce flavor-changing neutral current in neutrino interactions. Then, even for the SM interactions, both neutral and charged currents, the sterile neutrino can appear in the final state. For both cases, the scattering matrix element with Z/W mediator is suppressed by the active-sterile mixing θ_{as}, $\mathcal{M}^s_{Z/W} \approx \theta_{as}\mathcal{M}^{\rm SM}_{Z/W}$. The corresponding interference term is then of the order $\theta_{as}\mathcal{M}^{\rm SM}_{Z/W}\mathcal{M}_\phi$ where $\mathcal{M}_\phi$ is the scalar-mediated contribution. As indicated in Fig. 1, the contribution of these two contributions is roughly the same when explaining the Xenon1T excess, $|\mathcal{M}^{\rm SM}_{Z/W}|^2 \sim |\mathcal{M}^{as}_\phi|^2$. The interference term is then controlled by the active-sterile mixing θ_{as} and can be easily suppressed.

The sterile neutrino scenario has implementations in both neutrino oscillation [57–59] and dark matter [61,62]. The keV sterile neutrino discussed in this paper belongs to the dark matter category and hence is largely unconstrained by the neutrino oscillation experiments. The strongest constraint comes from meson decay experiments and for electron neutrino it is of order $|y^\nu_{S,P}| \lesssim 10^{-3}$

Please cite this article in press as: S.-F. Ge et al., Solar neutrino scattering with electron into massive sterile neutrino, Phys. Lett. B (2020), https://doi.org/10.1016/j.physletb.2020.135787

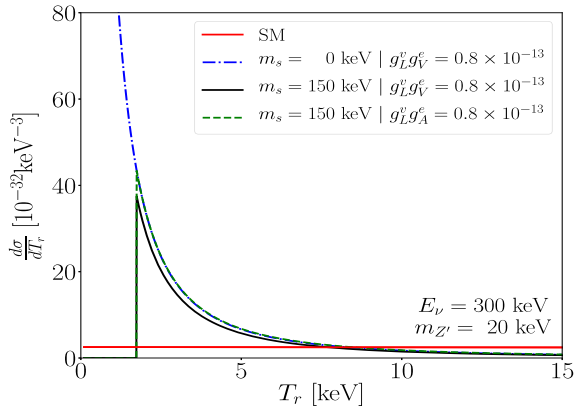

Fig. 4. The electron recoil energy spectrum for the SM background and sterile neutrino final state with scalar mediator.

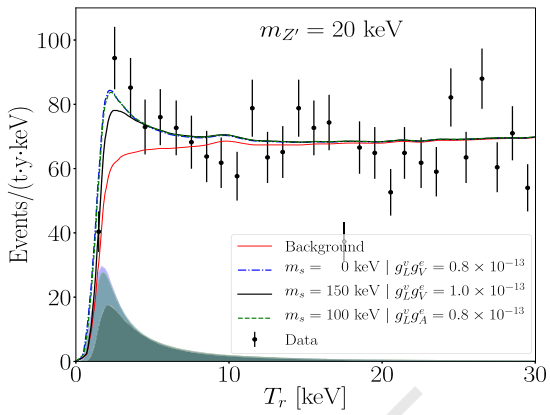

Fig. 5. The electron recoil event rate at Xenon1T.

[63–66]. At the same time, Big Bang Nucleosynthesis requires that $|y_S^e| \lesssim 5 \times 10^{-10}$ [67] if the scalar mediator is kept in thermal equilibrium with the primordial plasma before $T \sim 1$ MeV, which would decrease the deuterium abundance. The combined bound is $|y_S^\nu y_S^e| \lesssim 5 \times 10^{-13}$ which our parameter choice satisfies.

6. Vector mediator

The same scenario of sterile neutrino in the final state also works with a light vector boson mediator. Since the recoil energy gap arises from kinematics, its application is not limited to the scalar force.

For simplicity, we consider only the situation where Z' couples to the left-handed neutrinos,

$$\mathcal{L}_{\rm int} = g_L^\nu \overline{\nu} \gamma^\mu P_L \nu_s Z'_\mu + \overline{e}(g_V^e - g_A^e \gamma_5)\gamma^\mu e Z'_\mu. \tag{7}$$

On the other hand, the electron coupling can have either vector or axial-vector current coupling with Z'. The corresponding differential cross section is,

$$\frac{d\sigma}{dT_r} = \frac{(g_L^\nu g_{V,A}^e)^2}{2\pi E_\nu^2}\left[\frac{2m_e(2E_\nu^2 + T_r^2 - T_r(2E_\nu \pm m_e))}{(2T_r m_e + m_{Z'}^2)^2} - \frac{m_s^2(2E_\nu - T_r \pm m_e)}{(2T_r m_e + m_{Z'}^2)^2}\right], \tag{8}$$

where + (−) stands for vector (axial-vector) current interaction with non-vanishing $g_{V,A}^e$ (vanishing $g_{A,V}^e$), respectively. It is interesting to see that the combination of neutrino and electron couplings $(g_L^\nu g_{V,A}^e)^2$ appear as overall factors. The differential cross section has exactly the same functional form no matter Z' couples to electron with vector or axial-vector interactions. This is very different from the scalar versus pseudoscalar comparison. Since the neutrino energy E_ν is much larger than the electron recoil energy T_r, the numerators are insensitive to T_r and the two terms of (8) always have $1/T_r^2$ enhancement.

Fig. 4 shows the differential cross section as a function of the electron recoil energy T_r. As expected, the sterile neutrino mass m_s places a much less significant role than the scalar case, the two terms of (8) have roughly the same contribution. This can be clearly seen as the same shape of the three sterile neutrino curves. The only major difference between massive and massless sterile neutrinos is the suppressed spectrum at the lower end for the former case. This can lead to testable effect with better resolution, lower threshold, and higher efficiency. The event rate spectrum at Xenon1T is shown in Fig. 5. The combination of massive sterile neutrino and light vector mediator can also explain the Xenon1T excess.

7. Non-standard interactions

With light mediator coupled to both neutrino and electron, neutrinos can feel the matter effect that arises from the forward scattering with electron. This leads to nonstandard interactions for Z' mediator,

$$\epsilon_{es}^e = \frac{g_{V,A}^\nu g_{V,A}^e}{4\sqrt{2}G_F m_{Z'}^2} \sim g_{V,A}^\nu g_{V,A}^e \left(\frac{10^8}{m_{Z'}[\rm keV]}\right)^2. \tag{9}$$

For $m_{Z'} = 1 \sim 20$ keV and $g_{V,A}^\nu g_{V,A}^e = 10^{-13}$, the size of the NSI parameter is $\epsilon_{es}^e = 3.6 \sim 1500$ with $\epsilon_{es}^e \equiv g_{V,A}^\nu g_{V,A}^e/(V_{cc} m_{Z'}^2)$ and V_{cc} denoting the matter potential from W exchange. Previous works considered the diagonal elements ϵ_{ss}^e [68,69] or cosmological impacts of ultra-light mediators [70] but not the active-sterile off-diagonal element that we discuss here. For comparison, the current bound on the NSI with only active neutrinos favors a small value $|\epsilon_{ee}^e| \lesssim 0.05$ [71], but only for the part after subtracting a common diagonal contribution.

For scalar mediator, the matter effect appears as correction to the neutrino mass term [72–74]. With $m_\phi = 20$ keV, the scalar NSI parameters $\eta_{es} = 4 \times 10^{-17}$ ($\delta M \equiv y_{S,P}^\nu y_{S,P}^e/m_\phi^2$ and $\eta_{es} \equiv \delta M/\sqrt{\Delta m_{31}^2}$) is quite small. For a sizable vector NSI, the correction $E_\nu V_{cc} \epsilon_{es}$ is to the mass squared term $M_\nu M_\nu^\dagger$ while the matter potential for scalar is $M_\nu + \eta_{es}\sqrt{\Delta m_{31}^2}$. For roughly same size of scalar and vector NSI, $\epsilon_{es} V_{cc} \sim \eta_{es}\sqrt{\Delta m_{31}^2}$, the relative correction is $E_\nu \epsilon_{es} V_{cc}/M_\nu M_\nu^\dagger \gg \eta_{es}\sqrt{\Delta m_{31}^2}/M_\nu$ since the neutrino energy is much larger than the neutrino mass, $E_\nu \gg M_\nu$. Then, we can safely omit the scalar NSI in the parameter space considered in this paper.

So both the scalar and vector mediator cases are safe from the NSI constraints.

8. Conclusions

In contrary to the common expectation that pseudoscalar mediator cannot leave significant contribution to low recoil phenomena, we notice a massive final-state companion fermion can introduce $1/T_r$ enhancement even for pseudoscalar mediator. Although we propose this sterile neutrino option to explain the Xenon1T excess, the same scenario also applies for other situations such as a light relativistic DM scattering into a massive invisible fermion. This significantly enlarges the model spectrum. The sub-keV threshold detector for low recoil energy scan to testify the existence of massive companion particle is an interesting direction to pursue.

Please cite this article in press as: S.-F. Ge et al., Solar neutrino scattering with electron into massive sterile neutrino, Phys. Lett. B (2020), https://doi.org/10.1016/j.physletb.2020.135787

Declaration of competing interest

The authors declare that they have no known competing financial interests or personal relationships that could have appeared to influence the work reported in this paper.

Acknowledgements

SFG is grateful to the Double First Class start-up fund (WF220442604) provided by Shanghai Jiao Tong University.

References

[1] E. Aprile, et al., Observation of excess electronic recoil events in XENON1T, arXiv:2006.09721.
[2] A.E. Robinson, XENON1T observes tritium, arXiv:2006.13278 [hep-ex].
[3] K. Kannike, M. Raidal, H. Veermäe, A. Strumia, D. Teresi, Dark matter and the XENON1T electron recoil excess, arXiv:2006.10735 [hep-ph].
[4] B. Fornal, P. Sandick, J. Shu, M. Su, Y. Zhao, Boosted dark matter interpretation of the XENON1T excess, arXiv:2006.11264 [hep-ph].
[5] G.F. Giudice, D. Kim, J.C. Park, S. Shin, Inelastic boosted dark matter at direct detection experiments, Phys. Lett. B 780 (2018) 543–552, arXiv:1712.07126 [hep-ph].
[6] Q.H. Cao, R. Ding, Q.F. Xiang, Exploring for sub-MeV boosted dark matter from xenon electron direct detection, arXiv:2006.12767 [hep-ph].
[7] Y. Jho, J.C. Park, S.C. Park, P.Y. Tseng, Gauged lepton number and cosmic-ray boosted dark matter for the XENON1T excess, arXiv:2006.13910 [hep-ph].
[8] L. Su, W. Wang, L. Wu, J.M. Yang, B. Zhu, Atmospheric dark matter from inelastic cosmic ray collision in Xenon1T, arXiv:2006.11837.
[9] G. Choi, M. Suzuki, T.T. Yanagida, XENON1T anomaly and its implication for decaying warm dark matter, arXiv:2006.12348 [hep-ph].
[10] Y. Chen, J. Shu, X. Xue, G. Yuan, Q. Yuan, Sun heated MeV-scale dark matter and the XENON1T electron recoil excess, arXiv:2006.12447 [hep-ph].
[11] K. Harigaya, Y. Nakai, M. Suzuki, Inelastic dark matter electron scattering and the XENON1T excess, arXiv:2006.11938 [hep-ph].
[12] H.M. Lee, Exothermic dark matter for XENON1T excess, arXiv:2006.13183 [hep-ph].
[13] N.F. Bell, J.B. Dent, B. Dutta, S. Ghosh, J. Kumar, J.L. Newstead, Explaining the XENON1T excess with luminous dark matter, arXiv:2006.12461 [hep-ph].
[14] M. Du, J. Liang, Z. Liu, V. Tran, Y. Xue, On-shell mediator dark matter models and the Xenon1T anomaly, arXiv:2006.11949 [hep-ph].
[15] J. Smirnov, J.F. Beacom, Co-SIMP miracle, arXiv:2002.04038 [hep-ph].
[16] G. Paz, A.A. Petrov, M. Tammaro, J. Zupan, Shining dark matter in Xenon1T, arXiv:2006.12462 [hep-ph].
[17] M. Baryakhtar, A. Berlin, H. Liu, N. Weiner, Electromagnetic signals of inelastic dark matter scattering, arXiv:2006.13918 [hep-ph].
[18] U.K. Dey, T.N. Maity, T.S. Ray, Prospects of Migdal effect in the explanation of XENON1T electron recoil excess, arXiv:2006.12529 [hep-ph].
[19] L. Zu, G.W. Yuan, L. Feng, Y.Z. Fan, Mirror dark matter and electronic recoil events in XENON1T, arXiv:2006.14577 [hep-ph].
[20] D. McKeen, M. Pospelov, N. Raj, Hydrogen portal to exotic radioactivity, arXiv:2006.15140 [hep-ph].
[21] R. Primulando, J. Julio, P. Uttayarat, Collider constraints on a dark matter interpretation of the XENON1T excess, arXiv:2006.13161 [hep-ph].
[22] L. Di Luzio, M. Fedele, M. Giannotti, F. Mescia, E. Nardi, Solar axions cannot explain the XENON1T excess, arXiv:2006.12487 [hep-ph].
[23] C. Gao, J. Liu, L.T. Wang, X.P. Wang, W. Xue, Y.M. Zhong, Re-examining the solar axion explanation for the XENON1T excess, arXiv:2006.14598 [hep-ph].
[24] I.M. Bloch, A. Caputo, R. Essig, D. Redigolo, M. Sholapurkar, T. Volansky, Exploring new physics with O(keV) electron recoils in direct detection experiments, arXiv:2006.14521 [hep-ph].
[25] W. DeRocco, P.W. Graham, S. Rajendran, Exploring the robustness of stellar cooling constraints on light particles, arXiv:2006.15112 [hep-ph].
[26] J.B. Dent, B. Dutta, J.L. Newstead, A. Thompson, Inverse Primakoff scattering as a probe of solar axions at liquid xenon direct detection experiments, arXiv:2006.15118 [hep-ph].
[27] J. Buch, M.A. Buen-Abad, J. Fan, J.S.C. Leung, Galactic origin of relativistic bosons and XENON1T excess, arXiv:2006.12488 [hep-ph].
[28] F. Takahashi, M. Yamada, W. Yin, XENON1T anomaly from anomaly-free ALP dark matter and its implications for stellar cooling anomaly, arXiv:2006.10035 [hep-ph].
[29] R. Budnik, H. Kim, O. Matsedonskyi, G. Perez, Y. Soreq, Probing the relaxed relaxion and Higgs-portal with S1 & S2, arXiv:2006.14568 [hep-ph].
[30] G. Alonso-Álvarez, F. Ertas, J. Jaeckel, F. Kahlhoefer, L. Thormaehlen, Hidden photon dark matter in the light of XENON1T and stellar cooling, arXiv:2006.11243 [hep-ph].
[31] K. Nakayama, Y. Tang, Gravitational production of hidden photon dark matter in light of the XENON1T excess, arXiv:2006.13159 [hep-ph].
[32] H. An, M. Pospelov, J. Pradler, A. Ritz, New limits on dark photons from solar emission and keV scale dark matter, arXiv:2006.13929 [hep-ph].
[33] J. Bramante, N. Song, Electric but not eclectic: thermal relic dark matter for the XENON1T excess, arXiv:2006.14089 [hep-ph].
[34] N.F. Bell, V. Cirigliano, M.J. Ramsey-Musolf, P. Vogel, M.B. Wise, How magnetic is the Dirac neutrino?, Phys. Rev. Lett. 95 (2005) 151802, arXiv:hep-ph/0504134.
[35] N.F. Bell, M. Gorchtein, M.J. Ramsey-Musolf, P. Vogel, P. Wang, Model independent bounds on magnetic moments of Majorana neutrinos, Phys. Lett. B 642 (2006) 377–383, arXiv:hep-ph/0606248.
[36] A.N. Khan, Can nonstandard neutrino interactions explain the XENON1T spectral excess?, arXiv:2006.12887 [hep-ph].
[37] M. Chala, A. Titov, One-loop running of dimension-six Higgs-neutrino operators and implications of a large neutrino dipole moment, arXiv:2006.14596 [hep-ph].
[38] C. Boehm, D.G. Cerdeno, M. Fairbairn, P.A. Machado, A.C. Vincent, Light new physics in XENON1T, arXiv:2006.11250 [hep-ph].
[39] A. Bally, S. Jana, A. Trautner, Neutrino self-interactions and XENON1T electron recoil excess, arXiv:2006.11919 [hep-ph].
[40] D. Aristizabal Sierra, V. De Romeri, L. Flores, D. Papoulias, Light vector mediators facing XENON1T data, arXiv:2006.12457 [hep-ph].
[41] M. Lindner, Y. Mambrini, T.B. de Melo, F.S. Queiroz, XENON1T anomaly: a light Z', arXiv:2006.14590 [hep-ph].
[42] D.W.P. do Amaral, D.G. Cerdeno, P. Foldenauer, E. Reid, Solar neutrino probes of the muon anomalous magnetic moment in the gauged $U(1)_{L_\mu - L_\tau}$, arXiv:2006.11225 [hep-ph].
[43] M.D. Campos, W. Rodejohann, Testing keV sterile neutrino dark matter in future direct detection experiments, Phys. Rev. D 94 (9) (2016) 095010, arXiv:1605.02918 [hep-ph].
[44] V. Shtabovenko, R. Mertig, F. Orellana, New developments in FeynCalc 9.0, Comput. Phys. Commun. 207 (2016) 432–444, arXiv:1601.01167 [hep-ph].
[45] D.G. Cerdeño, M. Fairbairn, T. Jubb, P.A.N. Machado, A.C. Vincent, C. Bœhm, Physics from solar neutrinos in dark matter direct detection experiments, J. High Energy Phys. 05 (2016) 118, arXiv:1604.01025 [hep-ph].
[46] C. Giunti, C.W. Kim, Fundamentals of Neutrino Physics and Astrophysics, Univ. Pr., Oxford, UK, 2007, 710 pp., Errata.
[47] S.-F. Ge, NuPro: a simulation package for neutrino properties, link.
[48] L. Wolfenstein, Neutrino oscillations in matter, Phys. Rev. D 17 (1978) 2369–2374.
[49] Michele Maltoni, Alexei Yu. Smirnov, Solar neutrinos and neutrino physics, Eur. Phys. J. A 52 (2016) 87, arXiv:1507.05287.
[50] S.P. Mikheyev, A.Y. Smirnov, Resonance amplification of oscillations in matter and spectroscopy of solar neutrinos, Sov. J. Nucl. Phys. 42 (1985) 913, Yad. Fiz. 42 (1985) 1441;
S.P. Mikheev, A.Y. Smirnov, Resonant amplification of neutrino oscillations in matter and solar neutrino spectroscopy, Nuovo Cimento C 9 (1986) 17;
S.P. Mikheev, A.Y. Smirnov, Neutrino oscillations in a variable density medium and neutrino bursts due to the gravitational collapse of stars, Sov. Phys. JETP 64 (1986) 4, arXiv:0706.0454 [hep-ph].
[51] M. Wurm, Solar neutrino spectroscopy, Phys. Rep. 685 (2017) 1–52, arXiv:1704.06331 [hep-ex].
[52] F. Vissani, Solar neutrino physics on the beginning of 2017, Nucl. Phys. At. Energy 18 (1) (2017) 5–12, arXiv:1706.05435 [nucl-th].
[53] N. Vinyoles, A.M. Serenelli, F.L. Villante, S. Basu, J. Bergström, M. Gonzalez-Garcia, M. Maltoni, C. Peña-Garay, N. Song, A new generation of standard solar models, Astrophys. J. 835 (2) (2017) 202, arXiv:1611.09867 [astro-ph.SR].
[54] P. de Salas, D. Forero, S. Gariazzo, P. Martí nez-Miravé, O. Mena, C. Ternes, M. Tó rtola, J. Valle, 2020 global reassessment of the neutrino oscillation picture, arXiv:2006.11237 [hep-ph].
[55] F. Capozzi, E. Di Valentino, E. Lisi, A. Marrone, A. Melchiorri, A. Palazzo, Addendum to: global constraints on absolute neutrino masses and their ordering, arXiv:2003.08511 [hep-ph].
[56] E. Aprile, et al., XENON, Energy resolution and linearity in the keV to MeV range measured in XENON1T, arXiv:2003.03825 [physics.ins-det].
[57] C. Giunti, T. Lasserre, eV-scale sterile neutrinos, Annu. Rev. Nucl. Part. Sci. 69 (2019) 163–190, arXiv:1901.08330 [hep-ph].
[58] A. Diaz, C. Argü elles, G. Collin, J. Conrad, M. Shaevitz, Where are we with light sterile neutrinos?, arXiv:1906.00045 [hep-ex].
[59] S. Böser, C. Buck, C. Giunti, J. Lesgourgues, L. Ludhova, S. Mertens, A. Schukraft, M. Wurm, Status of light sterile neutrino searches, Prog. Part. Nucl. Phys. 111 (2020) 103736, arXiv:1906.01739 [hep-ex].
[60] A. de Gouvêa, O. Peres, S. Prakash, G. Stenico, On the decaying-sterile neutrino solution to the electron (anti)neutrino appearance anomalies, arXiv:1911.01447 [hep-ph].
[61] M. Drewes, et al., A white paper on keV sterile neutrino dark matter, J. Cosmol. Astropart. Phys. 01 (2017) 025, arXiv:1602.04816 [hep-ph].
[62] A. Boyarsky, M. Drewes, T. Lasserre, S. Mertens, O. Ruchayskiy, Sterile neutrino dark matter, Prog. Part. Nucl. Phys. 104 (2019) 1–45, arXiv:1807.07938 [hep-ph].
[63] P. Pasquini, O. Peres, Bounds on neutrino-scalar Yukawa coupling, Phys. Rev. D 93 (5) (2016) 053007, arXiv:1511.01811 [hep-ph].

[64] J.M. Berryman, A. De Gouvêa, K.J. Kelly, Y. Zhang, Lepton-number-charged scalars and neutrino beamstrahlung, Phys. Rev. D 97 (7) (2018) 075030, arXiv:1802.00009 [hep-ph].
[65] J.A. Dror, Discovering leptonic forces using nonconserved currents, Phys. Rev. D 101 (9) (2020) 095013, arXiv:2004.04750 [hep-ph].
[66] A. de Gouvêa, P.B. Dev, B. Dutta, T. Ghosh, T. Han, Y. Zhang, Leptonic scalars at the LHC, arXiv:1910.01132 [hep-ph].
[67] K.S. Babu, G. Chauhan, P.S. Bhupal Dev, Neutrino non-standard interactions via light scalars in the Earth, Sun, supernovae and the early Universe, Phys. Rev. D 101 (9) (2020) 095029, arXiv:1912.13488 [hep-ph].
[68] J. Liao, D. Marfatia, K. Whisnant, MiniBooNE, MINOS+ and IceCube data imply a baroque neutrino sector, Phys. Rev. D 99 (1) (2019) 015016, arXiv:1810.01000 [hep-ph].
[69] Jiajun Liao, Danny Marfatia, Impact of nonstandard interactions on sterile neutrino searches at IceCube, Phys. Rev. Lett. 117 (2016) 071802, arXiv:1602.08766.
[70] Y. Farzan, Ultra-light scalar saving the 3 + 1 neutrino scheme from the cosmological bounds, Phys. Lett. B 797 (2019) 134911, arXiv:1907.04271 [hep-ph].
[71] Y. Farzan, M. Tortola, Neutrino oscillations and non-standard interactions, Front. Phys. 6 (2018) 10, arXiv:1710.09360 [hep-ph].
[72] S. Bergmann, Y. Grossman, E. Nardi, Neutrino propagation in matter with general interactions, Phys. Rev. D 60 (1999) 093008, arXiv:hep-ph/9903517.
[73] J. Liao, D. Marfatia, K. Whisnant, Generalized perturbations in neutrino mixing, Phys. Rev. D 92 (7) (2015) 073004, arXiv:1506.03013 [hep-ph].
[74] S.F. Ge, S.J. Parke, Scalar nonstandard interactions in neutrino oscillation, Phys. Rev. Lett. 122 (21) (2019) 211801, arXiv:1812.08376 [hep-ph].